

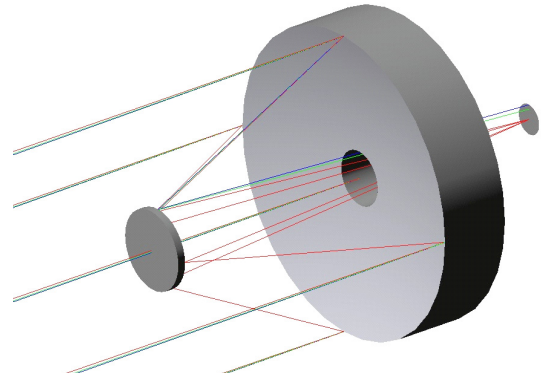
# DESIGN AND FABRICATION OF OPTICAL SYSTEMS

Nadim Wanna, Lucas Lamonds, Robert Woodside,  
Thomas Dow, Kenneth Garrard, Alexander Sohn  
Precision Engineering Center, North Carolina State University

## OPTICAL DESIGN

The goal of this project is to gain familiarity with optical design, fabrication and performance evaluation for telescope systems constructed from mirrors. For optical design, this means becoming acquainted with different types of optical systems, optical design software, aberrations associated with these systems, design conventions, limits of performance, basic sizing parameters and fabrication sensitivities. A system using two mirrors was selected for the first prototype because of the simplicity of the design and ease of fabrication, assembly and metrology.

**Ritchey-Chretien Design** This design was first introduced in a 1904 paper “On the Modern Reflecting Telescope, and the Making and Testing of Optical Mirrors”. It is a modification of the Cassegrain design and uses a two mirror layout shown at right. The primary mirror is the main light gatherer and is designed to focus light to a point. The secondary reflects this light to an observer behind the primary. In this configuration both aspheres are hyperbolic and correct simultaneously for spherical aberrations and coma. However, like the Cassegrain, the Ritchey-Chretien design is limited by astigmatism at high field angles. Ritchey-Chretien designs typically have an  $f$ -number (focal length/aperture diameter) range of 4 to 6 and full field angles of  $0.75^\circ$  to  $2^\circ$ .



**Specifications** The overall size of the optical system is determined by optical, fabrication and mechanical design issues. A primary aperture diameter of 150mm served as the design starting point. Because astigmatism is function of field height in all two-mirror designs, this system is restricted to a  $1^\circ$  field. The  $f$ -number, or speed, of the system was set by the aperture and detector size and was  $f/5.73$  for this prototype. The primary is  $f/1$  with a diameter of 150 mm, a focal length of 150 mm and radius of curvature of 300 mm. The conic constant was set to -1 (parabola) and allowed to vary and the primary had a 25 mm hole in the center. The size of the secondary is set by the height of the marginal ray from the primary and the conic constant was initially set to -3. The location of the secondary mirror (percentage of the secondary distance from the primary's focal point) influences the obscuration of the incoming beam and was initially set at 20%. The telescope was designed to support a Canon digital camera.

**Optimization** Global system specifications are used in CODE V® to initialize the system and solve basic system parameters. The entrance pupil is 150mm, or the size of the primary, and the analysis wavelength is 587.561 nm. Because this is a reflecting system; chromatic separation and aberrations are absent. Fields angles are  $0^\circ$  (axis),  $0.35^\circ$  (70% of half field height) and  $0.5^\circ$  (half field height). By using 70% as the middle field value, best focus optimization yields equal spot sizes for  $0^\circ$  and  $0.5^\circ$ . Paraxial Image Solve is enabled such that the image surface is at the system paraxial image focus, or the point where the rays parallel to the system axis converge. All specifications not explicitly selected are allowed to vary during optimization. Both mirrors are hyperbolas and the final conic constant of the primary is -1.0195 and the secondary is -2.166. Radius of curvature for the secondary is 88.1225 mm and the aperture diameter is 38.94 mm. The composite field best focus is 0.340 mm closer to the secondary. The center hole of the primary was increased to 26mm to allow full field rays through the hole. Secondary spacing was adjusted by trial and error to 24.25% or 113.625mm. As a result, the distance from the secondary to the image plane on the digital camera. The effective focal length of the finalized system is 859.872mm.

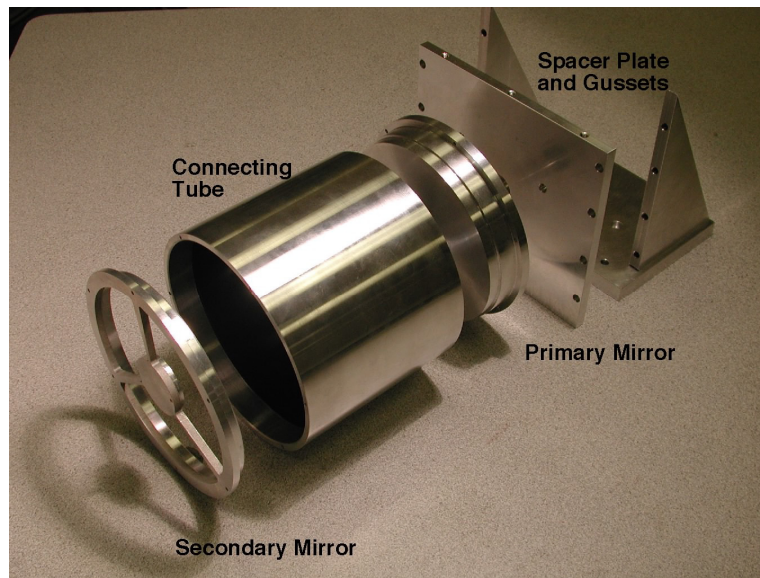
**Performance Prediction** When the optical design is created and optimized, the performance can be estimated with CODE V. A wide variety of parameters are available to determine the expected performance of the system and the source of the largest errors. Geometrical analysis can generate spot diagrams, radial energy analyses and detector

analyses and diffraction analyses can produce modulation transfer functions, point spread functions and wavefront error maps including the effects of spherical aberrations, coma, astigmatism and higher order components.

### OPTOMECHANICAL DESIGN

The design of the structure to support the imaging optics is extremely important. Design issues are as follows: mechanical support of the mirrors in the system to keep the image quality within specification, assembly fiducials and material selection. The different telescope components, shown at right are the primary mirror, secondary mirror, secondary connecting tube, spacer, gussets, and base plate.

Several different designs of the crucial connection between the primary and secondary mirror were considered. The tube design shown at right is the simplest. A cylindrical surface on the primary mirror locates the axis of the tube to be coincident with the axis of the primary and the stop sets the distance along that axis. The secondary also has a cylindrical surface with stop to locate the secondary. The length of the tube determines the distance between the primary and secondary.



All the components of the telescope are Aluminum 6061-T6. This material combines relatively high strength, low weight, good machinability with diamond tools, excellent coating adhesion and high resistance to corrosion. Also, by using a single material, distortion of the components due to an environmental temperature change is minimized.

**Effect of Manufacturing Errors on Optical Performance** After being rough machined and heat treated, the optical and fiducial surfaces are diamond turned to optical shape and surface finish. The desired theoretical finish of the fiducial surfaces is 10 nm, while the theoretical finish on the mirror surfaces is 1nm. The tolerance of having a part width or length fabricated on the diamond turning machine is  $\pm 1 \mu\text{m}$ . The fiducial surfaces of the system are finished by diamond turning to insure that the distance from the back surface of the primary to the apex of the secondary mirror is within the specified tolerance. A second key dimension is the distance from the camera's mounting surface to the back of the primary mirror.

Precision machining should guarantee sufficiently accurate location of the fiducial surfaces such that the optical performance will be as predicted from the Code V analysis. The analysis revealed individual errors increase by 0.045 RMS waves or less for each field angle. The cumulative probability for each field angle was calculated and the maximum value at the marginal ray was equal to  $0.8 \lambda$ . This probability is based on a  $2\sigma$  Gaussian distribution. The wavefront error is degraded by 70% at the optimized field angle of  $0.35^\circ$  for the selected fabrication tolerances.

### FABRICATION

The telescope components were rough machined with allowances for final machining on the optical and fiducial surfaces. Each of these surfaces has at least  $150 \mu\text{m}$  of extra material that is removed during final machining. The optical surfaces were compared to their spherical equivalents and the extra sag was added to the  $150 \mu\text{m}$ . The taper press fit has  $150 \mu\text{m}$  of material plus the taper angle material. After rough machining, the components were heat treated using a series of cooling/heating cycles between  $-100^\circ \text{F}$  and  $300^\circ \text{F}$ .

The order for diamond turning of the machined components is as follows:

- **Primary** The shape of the primary mirror is a 150 mm diameter hyperbola with a 26 mm hole. The apex location is referenced to the back of the mirror. The back of the mirror will first be diamond turned and a spherical feature will be machined on the edge of the hole. This will be used to find the center of the primary in the dual pass interferometer measurements discussed later. The mirror will be vacuumed to the DTM spindle

and the 5 mm nose radius diamond tool will “touch” the chuck surface to set the reference z dimension. The programmed path will be a series of x,z commands that are based on the mathematical description of the hyperbolic optical surface. The surface will be machined to the proper hyperbolic shape with increasing depth until the desired 25 mm spacing between apex and back surface has been achieved. The fiducial feature that transfers the primary optical shape to the secondary is a step on the OD that mates with the tube. The crucial features of this fiducial are the taper angle ( $1^\circ$ ), the diameter and the axial distance to the back surface of the mirror. These features will be machined with a second diamond tool (“dead sharp”) that will be centered (x reference) and set to z reference by touching off on the vacuum chuck.

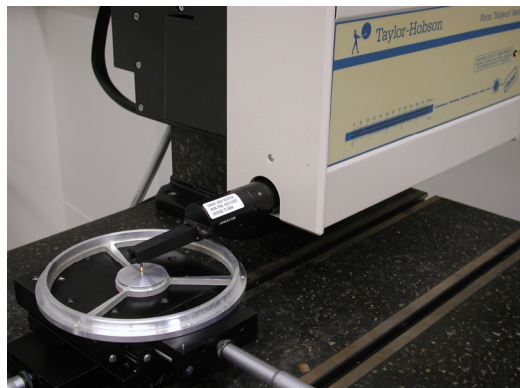
- **Secondary** The secondary mirror is another hyperbolic surface but is much smaller (~40 mm diameter) and is convex rather than concave. The optical surface is supported on three arms to an outer ring that mates with the other end of the tube from the primary. As with the primary, the optical surface and the fiducial stops are machined on the DTM. The space between the outside ring and the optical surface (between the support arms) is covered with a thin plate to provide a vacuum seal.
- **Tube** The tube provides the connection between the primary and secondary mirrors. It sets the axial spacing as well as aligning the two optical axes to be coincident. The ID of each end includes an interference fit surface with an axial seating surface. These surfaces mate to the primary and the ring on the outside of the secondary, respectively.

## METROLOGY

There are many existing techniques to test optical systems that take into account both the system as a whole and the individual components. Examples of methods for testing the whole system are Modulation Transfer Functions (MTFs), various optical targets, dual pass interferometry and power loss analysis. Methods for testing individual components include profilometry, shape measuring interferometry and coordinate measuring machines.

### Individual Component Measurements

**Profilometry** The shape of the individual mirrors can be measured with a stylus profilometer. Typical profilometers have a contacting stylus that can be translated across the face of the component as shown at right. A laser interferometer records the vertical motion of the probe which can be combined with the horizontal position to create a profile of the optical surface. The profilometer has an advantage over optical instruments because the measured surface does not need to be reflective. This allows the components to be measured at stages prior to the final diamond turning. However, the disadvantage of the profilometer is that it is contacting measurement and damage to the surface is possible. The horizontal range of motion of the Talysurf is 120 mm (resolution of 20  $\mu\text{m}$ ) and the vertical range is 12 mm (resolution of 10 nm).



**Interferometry** Another method of determining the form of a reflective optical component is phase-shifting interferometry. This technique compares the wavefront from a reference sphere or flat to that reflected from the surface of a flat or spherical optical component. The interference between these two beams creates a fringe pattern that represents the difference between them. For a particular fringe pattern, there is some ambiguity in the shape of the surface so multiple measurements are made by moving the reference surface in known steps (phase shifting interferometry) and creating an optical path difference (OPD) for the surface compared to the best fit sphere. This measurement is only as good as the reference surface because the measurement is a comparison of these two surfaces. Interferometry is useful because it can be used to measure larger components than the profilometer and because it is non-contacting. However, it is only able to measure reflective surfaces and can therefore only be useful on a finished product.

### System Measurements

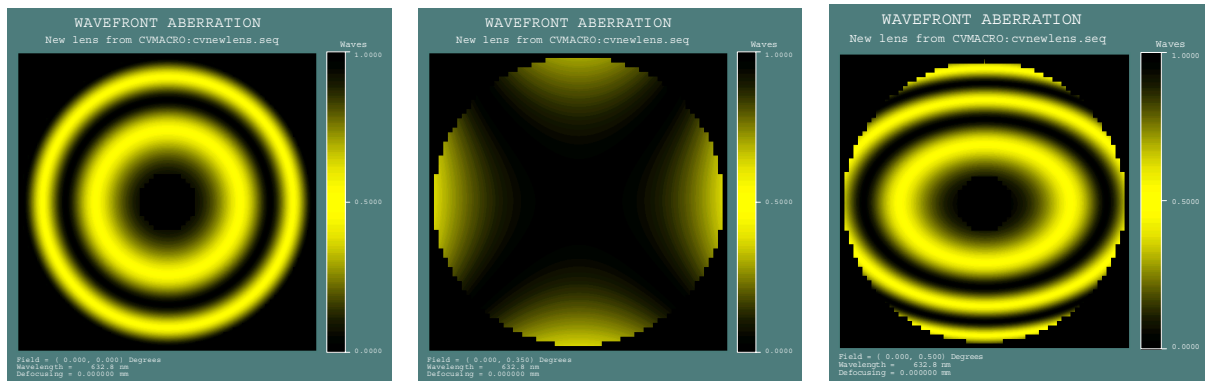
The shape of the individual components must give way to system performance measurements once the components are assembled. Several techniques are being evaluated to provide a measurement of the system.

**Dual-Pass Interferometer** The entire optical system will be tested using a double-pass interferometer. The telescope will be mounted on a linear/tilt stage on the intermediate stage of a Zygo GPI interferometer shown at right. A spherical wavefront will be focused on the detector plane above the back of the primary mirror. A narrow spherical mirror surface machined on the ID of the hole in the primary will be used to center the telescope in the GPI beam. Because the detector plane is at the focus of the secondary mirror, the light from the interferometer will be reflected onto the primary mirror and produce a linear wavefront out of the front of the telescope. A flat reflector, also on a tip/tilt stage, will be placed on the bottom of the vertical frame to reflect the light back through the telescope and into the interferometer. A perfect telescope and reflector will generate no fringe patterns in the interferometer.



The dual pass interferometer will allow the complete telescope to be measured including the shape and the location of the mirrors. Errors in either will show up as a wavefront error in the interferogram. By creating synthetic interferograms for the expected errors in the telescope (for example wavefront errors at different field angles shown below), the system performance can be measured and an estimate of the error source can be determined. To measure the performance at different field angles, the telescope is laterally shifted and the flat mirror at the bottom is tilted to the off-axis locations.

Other specific fabrication errors can also be evaluated by forcing misalignment of one component with respect to another. For example, the secondary mirror can be moved axially and the interference image can be predicted in Code V and measured in the dual-pass interferometer. Possible methods for translating the secondary mirror include hanging small weights and inserting a screw from the side to push on the mirror. Each of these methods will produce known deflections that can be used to produce off-axis rays comparable to those produced in the Code V software. The software on the Zygo GPI (MetroPro) can also create Modulation Transfer Functions, Point Spread Function and general wavefront error plots. Code V produces similar plots and the two can be compared. Code V can also create plots for both on and off-axis beams as illustrated below. These expected shapes can be compared to the measurements for the tilted telescope discussed above to obtain a full characterization of the optical system. The wavefront error data can also be inserted directly into the Code V software to produce a reference surface. This imported surface can be compared with the expected surface produced by Code V to derive the experimental error.



## CONCLUSIONS

The telescope design described here is the first in a series of optical systems that are being created to address the infrastructure issues that inhibit the adoption of freeform surfaces. This system is not a freeform design and in fact is a rotationally symmetric design whose major complication is its hyperbolic shapes. However, it allows the issues of design, fabrication, metrology and assembly to be addressed in a simple geometry and will serve as a basis for more complicated designs such as Three Mirror Anastigmats with off-axis aspheres and true freeform surfaces that come next.